journal

J. Am. Ceram. Soc., 79 [2] 385–94 (1996)

# Synthesis of Yttrium Aluminum Garnet from Yttrium and Aluminum Isobutyrate Precursors

Yin Liu, Zhi-Fan Zhang,* Bruce King,* John Halloran,* and Richard M. Laine*

Department of Materials Science and Engineering, University of Michigan, Ann Arbor, Michigan 48109-2136

**Mixtures of yttrium and aluminum isobutyrates, $M(O_2CCHMe_2)_3 = M(O_2CiPr)_3$ (M = Y or Al), were examined as precursors for processing yttrium aluminum garnet (YAG, $Al_5Y_3O_{12}$). Both precursors were synthesized by reacting the respective metal with isobutyric acid. The individual compounds and the $5Al(O_2CiPr)_3$:$3Y(O_2CiPr)_3$ YAG composition mixture were characterized by TGA, DTA, XRD, NMR, and FTIR. Pyrolytic decomposition of $Al(O_2CiPr)_3$ at temperatures ≤700°C produces amorphous $Al_2O_3$, which partially crystallizes to η-alumina at 840°C (by DTA), and finally to α-alumina at 1120°C. The pyrolysis behavior of $Y(O_2CiPr)_3$ is quite different. Samples start to decompose at 260°C, producing mixtures of $Y_2O_3$ with minor quantities of a yttrium carbonate species. On further heating to 300°C, the amorphous $Y_2O_3$ crystallizes (bcc). The carbonate remains stable until ≈900°C, and phase-pure, bcc $Y_2O_3$ is obtained only on heating to 1400°C. Mixtures of $Al(O_2CiPr)_3$ and $Y(O_2CiPr)_3$ provide a precursor to polycrystalline YAG. Rheologically useful solutions are obtained by dissolving a 5:3 mixture of $Al(O_2CiPr)_3$ and $Y(O_2CiPr)_3$ in THF. Solvent removal provides bulk samples of the YAG precursor. The pyrolytic decomposition patterns of bulk samples of this YAG precursor were studied by heating to selected temperatures and characterizing by TGA, DTA, XRD, and FTIR. The crystallization behavior of the mixture is quite different from the constituent compounds. The precursor decomposes to an amorphous material on heating above 300°C. On continued heating (5°C/min/air) this amorphous intermediate crystallizes (≈910°C) to phase-pure YAG with a final ceramic yield of 26% at 1000°C. No other phases are observed to form over this temperature range.**

## I. Introduction

YTTRIUM ALUMINUM GARNET (YAG or $Al_5Y_3O_{12}$) finds frequent application because of its good optical properties. Recent work shows that it also has great potential as a high-temperature engineering material, due to its high-temperature strength coupled with low creep rates.[1–4] For example, Corman's work on compressive creep of single-crystal YAG shows that at 1700°C and at an applied stress of 100 MPa, the creep rate is $2 \times 10^{-9}$ s$^{-1}$.[1] Under analogous conditions, single-crystal $Al_2O_3$ creeps at a rate of $2 \times 10^{-8}$ s$^{-1}$.[1] Unfortunately, single-crystal YAG is costly and technically difficult to produce because of its high melting point (1970°C).[2] One potential alternative is fine-grained (≤3 μm) polycrystalline YAG, which can be made economically and also exhibits good high-temperature properties. At 1400°C, polycrystalline YAG (≈3 μm grain size) stressed at 75.5 MPa, exhibits a creep rate of $2.5 \times 10^{-6}$ s$^{-1}$, which is lower than the $7.5 \times 10^{-6}$ s$^{-1}$ found for polycrystalline $Al_2O_3$ (≈3 μm grain size).[3,4] These properties suggest that polycrystalline YAG could supplant α-$Al_2O_3$ for a wide variety of applications, especially as reinforcing fibers in high-temperature composites, providing good processing methods can be developed (e.g., to provide precise control of grain sizes and size distributions).

Unfortunately, traditional ceramic (e.g., powder and melt) processing methods usually require high temperatures and lengthy heat treatments to obtain the homogeneity necessary to produce phase-pure YAG. These processing conditions do not permit facile control of microstructure, grain size, and grain size distribution, in the resulting ceramic shapes. Moreover, traditional methods are not amenable to processing thin fibers (<50 μm diameter) or films. These shapes are only available via chemical processing routes to YAG. Ceramic materials processed by metalloorganic (e.g., metal carboxylate) or sol–gel methods[5] offer access to optimal stoichiometry, atomic mixing, low phase transformation temperatures, and therefore, control of microstructure.[6]

Of the two chemical approaches to ceramic materials, the metalloorganic preceramic processing route offers some advantages over sol–gel processing. First, in sol–gel processing, the rheological properties necessary for fiber spinning require *in situ* creation of chemical cross-links via hydrolysis of alkoxide precursors and subsequent condensation of the hydrolytically generated intermediates. Close control of both reactions is critical to realizing the relatively narrow window of conditions wherein good spinnability obtains. Beyond this processing window, intractable gels can result.

In contrast, metalloorganic precursors rely on preformed bonding arrangements in the polymer, solvent selection, and polymer concentration for rheological control.[6] Their rheological properties are controlled by hydrogen and electrostatic bonding, and mechanical cross-linking interactions rather than hydrolytically induced chemical (covalent) cross-linking. For this reason, metalloorganic precursor solutions are more suitable for fiber spinning and can generally be stored for long periods of time, without forming intractable gels.

Secondly, YAG is a multimetallic oxide. Metalloorganic processing readily provides more effective atomic mixing of multimetallic systems than sol–gel processing, unless special precautions are taken. In sol–gel processing, different component metal alkoxides can have extremely different rates of hydrolysis; hence the method often cannot achieve effective atomic mixing and homogeneity in the final product.[7–11] Recent work by a number of groups has demonstrated that it is possible to modify the hydrolysis rates of a given alkoxide in a multimetallic alkoxide mixture, through use of chelating ligands or the formation of double alkoxides, to minimize segregation in the final product.[8,12,13] However, these modified versions still depend on gelation to preserve atomic mixing; thus, the first criterion of spinnability is still difficult to meet. In contrast, atomic mixing and processability in metalloorganic precursors rely on intermolecular bonding interactions between ligands, without hydrolysis. Atomic mixing of the metal components

C. J. Brinker—contributing editor

Manuscript No. 193693. Received April 5, 1994; approved November 14, 1994.
Supported by the U.S. Air Force Wright Laboratory, Wright Patterson Air Force Base, through Contract No. F33615-91-C-5650.
*Member, American Ceramic Society.

can be expected to be uniform providing all the components dissolve completely in a suitable solvent.

Metalloorganic polymer processing has some problems, such as (1) effective removal of carbon-containing ligands to minimize carbon impurities, and (2) the densification and accompanying volume changes that occur during formation of ceramic materials.[6] Because the organic ligands must be removed, preceramic polymers always have much lower densities than the target ceramic products. However, for thin films and fibers, the significant volume changes associated with metalloorganic processing are not a serious problem, because (1) little or no mass transport and shrinkage occur in at least one dimension (in fibers, the axial dimension), which helps retain shape integrity, and (2) the diffusion distances for mass transport are very short in other directions (in fibers, the diametrical direction), so that gaseous byproducts are removed easily and the ceramic residues readily densified during pyrolysis.

We have previously shown that metal carboxylates, especially the relatively low carbon content isobutyrates, permit facile processing of metalloorganic precursor fibers.[6,14] Furthermore, they are easily synthesized. Thus, we chose to explore the utility of 5:3 mixtures of Al and Y isobutyrates as precursors to polycrystalline YAG.

In this paper, we describe (1) the syntheses of the Al and Y isobutyrates, $Al(O_2CiPr)_3$ and $Y(O_2CiPr)_3$, (2) their reactivity patterns, and (3) the reactivity patterns of 5:3 (Al:Y) stoichiometric mixtures of these compounds during their respective pyrolytic transformation to phase-pure $Al_2O_3$, $Y_2O_3$, and YAG. Details on fiber processing will be presented at a later date.

## II. Experimental Procedures

### *(1) General Procedures*

Isobutyric acid (99%) was purchased from Pfaltz and Bauer Inc. Isobutyric anhydride (97%) was purchased from Aldrich Chemical Co. Toluene, THF (Mallinckrodt Co.), and MeCN (J. T. Baker) were distilled from the appropriate drying agents under $N_2$ and stored under $N_2$ prior to use. Aluminum powder (<8 mesh, Allied Chemical and Dye Co.) and Y chips (Morton Thiokol, Inc.) were used as received. All reactions were run under $N_2$ in standard Schlenkware.[6]

### *(2) Synthesis of Aluminum Isobutyrate, $Al(O_2CiPr)_3$*

(1) A mixture of 2.4 g (88 mmol) of Al powder, 70.0 mL (755 mmol, ≈2.9 equiv) of isobutyric acid, 2.0 mL (12 mmol) of isobutyric anhydride, and 200 mL of toluene (as solvent) were mixed with a catalytic amount of $HgCl_2$ (≈0.1 g, 0.4 mmol) in a 500 mL Schlenk flask. The mixture was then heated to reflux with stirring. The color of the reaction solution changed to dark gray as Al powder was consumed. (2) The solution was allowed to react for 4 days, then cooled and filtered through a medium-size frit. The recovered solid was collected and recycled. (3) The filtrate was filtered again through celite to give a clear solution. Solvent was removed by vacuum evaporation at 120°C to give off-white $Al(O_2CiPr)_3$ (11.4 g, 46% yield). (4) The recovered mixture of toluene and other liquid residuals (e.g., anhydride) was then mixed with the recovered solid filtered from the synthesis reaction. The mixture was then heated and stirred at reflux to dissolve a further portion of the recovered solid. An additional 2.35 g of product was obtained, by repeating steps (2) and (3) to give a net yield of 55%. The product is THF soluble; however, if the filtered THF solution is exposed to air, it rapidly becomes cloudy, indicating moisture sensitivity.

### *(3) Syntheses of Yttrium Isobutyrate, $Y(O_2CiPr)_3$*

Yttrium metal shavings (12.7 g, 143 mmol) were placed in a Schlenk flask with 60 mL (650 mmol) of isobutyric acid (1.5 equiv), 2.0 mL (12 mmol) of isobutyric anhydride, 200 mL of THF, and 0.10 g (0.4 mmol) of $HgCl_2$ as catalyst. The mixture was refluxed under $N_2$ until no further $H_2$ evolution (≈24 h) was observed. The hot solution was filtered through celite and allowed to cool. The product, $Y(O_2CiPr)_3$, precipitated out of solution on addition of 200 mL of dry MeCN. After washing three times with 100 mL of MeCN, the product was vacuum dried at 120°C, for 2 h. The white solid product was ground into a powder with alumina pestle and mortar. The yield was 34 g (97 mmol, 70% of theory).

### *(4) YAG Precursor Solution*

A 5:3 stoichiometric precursor solution ($5Al(O_2CiPr)_3$:$3Y(O_2CiPr)_3$, was formulated by dissolving 7.54 g (21.5 mmol, 43 wt%) of $Y(O_2CiPr)_3$ and 10.0 g (38.5 mmol, 57 wt%) of $Al(O_2CiPr)_3$ in 100 mL of THF. Isobutyric acid (≈0.2 mL) was added to aid dissolution. The yttrium isobutyrate used was 10% less than the formula ratio because 10% of the Al isobutyrate was insoluble in the THF. The solution was filtered to remove the small amount of insoluble matter. The solvent volume was then reduced by vacuum evaporation at 70°C to give dry powders suitable for bulk pyrolysis studies and density measurements.

### *(5) Density Measurements*

Density measurements were used to establish the theoretical volume changes expected during conversion of precursor to ceramic. The $Al(O_2CiPr)_3$, $Y(O_2CiPr)_3$, and YAG precursor were ground in the glove-box and the powders were removed and rapidly pressed into 1.28 cm diameter cylindrical pellets with an applied pressure of $1.5 \times 10^4$ Pa for 15 s. The carboxylate complexes deform plastically. The resulting pellet is assumed to be nearly 100% dense.[6] Calipers were used to measure the dimensions of compacted pellets to determine the densities.

### *(6) Pyrolysis Studies*

Ground samples (≈1 g) of $Al(O_2CiPr)_3$, $Y(O_2CiPr)_3$, and YAG precursor were placed in separate $Al_2O_3$ boats, and heated in dry air at 5°C/min to 300°, 500°, 700°, 800°, 900°, 1000°, or 1400°C for 2 h in a Thermolyne Type 6000 furnace (Barnstead Thermolyne Co., Dubuque, IA).

### *(7) Thermogravimetric Analyses (TGA)*

TGA studies were conducted using a Hi-Res TGA 2950 thermogravimetric analyzer, TA Instruments Thermal Analyst 2200 (TA Instruments, Inc., New Castle, DE). Samples (10–30 mg) were heated in a Pt pan, in dry air, at 5°C/min to 1000°C with an air flow rate of 60 $cm^3$/min.

### *(8) Differential Thermal Analyses (DTA)*

DTA experiments were conducted on a DSC 2910 differential scanning calorimeter (TA Instruments, Inc., New Castle, DE). Samples (≈10–20 mg) were loaded in a Pt crucible and heated at 5°C/min to 1500°C in dry air at a flow rate of 50 $cm^3$/min. The DTA reference was α-alumina (Aluminum Co. of America, Pittsburgh, PA).

### *(9) Diffuse Reflectance Infrared Fourier Transform Spectroscopy (DRIFTS)*

DRIFTS studies were performed using a Mattson Galaxy Series FTIR-3000 (Mattson Instruments, Inc., Madison, WI). Samples were prepared in a glove-box ($N_2$ environment) using crystalline KBr. The KBr was optical-grade random cuttings commercially available from International Crystal Laboratories (Garfield, NJ). The KBr was ground in a mortar and pestle, and 600 mg was weighed out. Then a 3.6 mg sample (0.6 wt% of KBr) was placed in a mortar and pestle, and ground. Approximately the same amount of KBr was added and the mixture was ground thoroughly. The remaining KBr was added in successive portions to approximately double the total amount of material in the mortar. Each addition was followed by thorough grinding. Finally, the sample was transferred to the IR sample holder and quickly placed in the IR sample chamber, which was kept under constant $N_2$ purge. The chamber was flushed with $N_2$ for at least 10 min before data collection. A minimum of 64 scans were collected for each sample at ±4 $cm^{-1}$ resolution. IR peak positions were identified using a standard peak searching program.

### *(10) NMR Characterization of Precursors*

The nulcear magnetic resonance (NMR) spectra were obtained on a Brüker Aspect 3000 AM-360 NMR (Brüker Instruments, Inc., Manning Park, Billerica, MA) spectrometer operated at 360 ($^1$H) or 90.6 ($^{13}$C) MHz using 30° pulse widths and relaxation delays of 1.0 ($^1$H) and 0.5 ($^{13}$C) s. $Y(O_2CiPr)_3$ and $Al(O_2CiPr)_3$ samples were dissolved in DMSO-$d_6$ (Aldrich Chemical Co., Milwaukee, WI) under Ar.[6] All signals were referenced to TMS (Aldrich).

### *(11) XRD Studies of Precursor Pyrolysis Products*

XRD was used to follow the pyrolytic transformation of the precursors to crystalline products, as a function of processing temperature, using a Rigaku rotating anode goniometer (Rigaku Denki Co. Ltd., Tokyo, Japan). Samples (40–80 mg) were prepared in a manner identical to that used for the DRIFTS samples. The powders were then loaded in sample holders (glass plates) for data collection. The working voltage and current were 40 kV and 100 mA, respectively. Cu$K\alpha$ ($\lambda$ = 1.54 Å) radiation with a Ni filter was used. Scans were continuous from 5° to 80° 2$\theta$ with a step scan of 10° 2$\theta$ per minute and increments of 0.05° 2$\theta$. The products, their peak positions, and the relative intensities were characterized by comparing with standard JCPDS files.

## III. Results and Discussion

In this section, we will discuss (1) the synthesis and characterization of the $Al(O_2CiPr)_3$, $Y(O_2CiPr)_3$, and a 5:3 (YAG composition) mixture of the two isobutyrates, (2) the pyrolytic reactivity patterns of the individual compounds, and (3) the pyrolytic decomposition patterns of the YAG precursor.

### *(1) Synthesis of $Al(O_2CiPr)_3$*

Aluminum isobutyrate was synthesized as follows:

$$Al + 3Me_2CHCO_2H \xrightarrow{THF/toluene/trace\ HgCl_2/reflux\ in\ N_2} 1.5H_2\uparrow + Al(O_2CiPr)_3 \quad (1)$$

To minimize hydrolysis of the $Al(O_2CiPr)_3$ product, e.g., via reaction (2), isobutyric anhydride was added to remove any adventitious $H_2O$ in the reaction environment.[6,14] Despite this precaution, the product from reaction (1) was always contaminated with a slight amount of $Al(OH)(O_2CiPr)_2$, as discussed in the DRIFTS section, which could derive from the aluminum hydroxide scale on the Al powder surface, as confirmed by direct reaction of $Al(OH)_3$ with isobutyric acid and anhydride (3).

$$Al(O_2CiPr)_3 + H_2O \rightarrow Me_2CHCO_2H + Al(OH)(O_2CiPr)_2 \quad (2)$$

$$Al(OH)_3 + 2(Me_2CHCO)_2O \rightarrow 2Me_2CHCO_2H + Al(OH)(O_2CiPr)_2 \quad (3)$$

Alternately, as suggested by a referee, the oxophilic character of the aluminum complex is such that it may compete successfully with anhydride as illustrated in reaction (4).

$$Al(O_2CiPr)_3 + Me_2CHCO_2H \rightarrow Al(OH)(O_2CiPr)_2 + (Me_2CHCO)_2O \quad (4)$$

We agree that this is a valid alternative, given the hydrolytic sensitivity of the complex, as discussed below.

### *(2) Characterization of $Al(O_2CiPr)_3$*

*(A) Thermal Analyses:* Based on our previous studies of isobutyrates, $Al(O_2CiPr)_3$ was expected to decompose primarily to the oxide at ≈400°C:[6]

$$Al(O_2CiPr)_3 \xrightarrow{\approx 400°C} Al_2O_3 + Al\ carbonate\ (traces) + gaseous\ byproducts\uparrow \quad (5)$$

The TGA profile for $Al(O_2CiPr)_3$ decomposition (Fig. 1) shows two mass loss processes, first from room temperature to 90°C, and second from 180° to 360°C, with a final 19% ceramic yield. The first process arises because of hydrolysis,[15,16] as determined by a TGA experiment run at room temperature in air. A sample of $Al(O_2CiPr)_3$ was found to lose 16% of its original mass in 6 h, simply as a result of its brief exposure to air during the time it was weighed into the TGA sample pan. The mass loss is explained by the evaporation of isobutyric acid formed by hydrolysis of $Al(O_2CiPr)_3$, reaction (2). The second mass loss arises because of oxidative decomposition of the organic ligands primarily to $CO_2$ and $H_2O$. The corresponding DTA (Fig. 2) exhibits a broad exotherm in the range 270–370°C.

The ceramic yield is slightly higher than calculated (18%) based on the formula, $Al(O_2CiPr)_3$, and reaction (5). The presence of an OH band in the DRIFT spectrum (see DRIFTS section) suggests that the slightly higher ceramic yield is due to some $Al(OH)(O_2CiPr)_2$ produced via reactions (2), (3), and/or

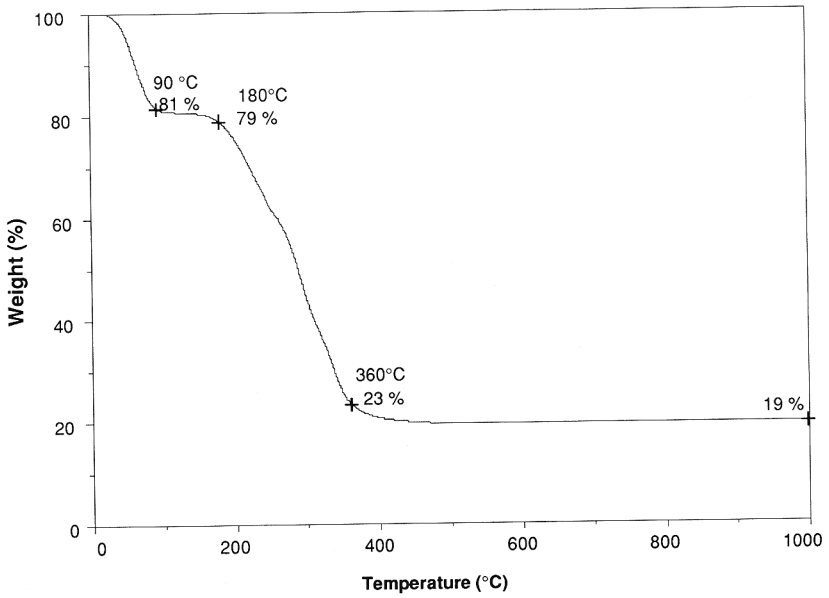


**Fig. 1.** TGA of aluminum isobutyrate. Samples were heated at 5°C/min in air to 1000°C.

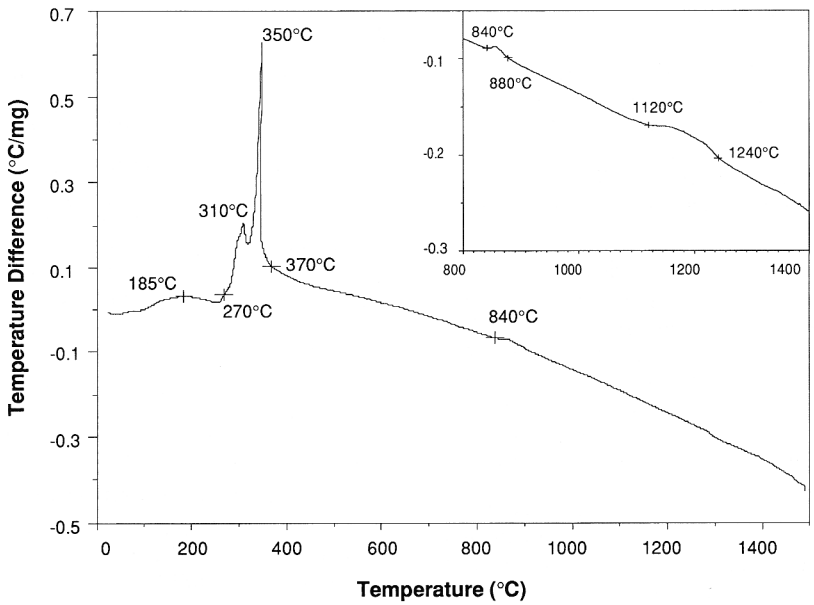


**Fig. 2.** DTA of aluminum isobutyrate. Samples were heated at 5°C/min in air to 1500°C.

(4). The theoretical ceramic yield for $Al(OH)(O_2CiPr)_2$ is 23%. Thus, the ceramic yield for our precursor can be anticipated to be slightly greater than expected for $Al(O_2CiPr)_3$ alone.

The Fig. 2 DTA does not provide details about high-temperature phase transformations because the sample size above 400°C is too small to compare with the reference, $Al_2O_3$ (at 400°C, the sample is ≈4 mg, 20% of its initial weight). DTA analyses require that the sample weight approximate that of the reference to optimize observed temperature differences. For this reason, a precursor sample was first pyrolyzed to 500°C for 2 h. Then the same quantity of sample and reference (usually 20 mg each) was used to run the DTA (5°C/min/air) to 1400°C to obtain the inset in Fig. 2. The inset shows two phase transformations, at 840–880°C and at 1120–1240°C. The XRD data for $Al(O_2CiPr)_3$ (Fig. 3) suggests that the 840–880°C exotherm corresponds to amorphous alumina transforming to η-alumina, while the 1120–1240°C exotherm corresponds to crystallization of α-alumina.

*(B) X-ray Powder Diffraction (XRD) Patterns:* Figure 3, the XRD data for $Al(O_2CiPr)_3$ heated to selected temperatures for 2 h in air (heating rate 5°C/min), shows that the material remains amorphous from 300° to 800°C. At 900°C, the powder pattern reveals low-intensity, broad peaks indicative of partial crystallization of η-alumina. Following heating to 1000°C, the peaks sharpen and grow in intensity as crystallization continues. At 1100°C, as supported by the DTA data (Fig. 2), α-alumina begins to crystallize. However, a well-defined α-alumina XRD pattern results only following heating to 1400°C.

*(C) DRIFTS:* Detailed IR analyses of various metal isobutyrate precursors, excluding $Al(O_2CiPr)_3$, are reported in Ref. 6. The $Al(O_2CiPr)_3$ spectra shown in Fig. 4 and the data recorded in Table I were analyzed by comparison with published data.[6,17–29] The antisymmetric $\nu_{C=O}$ band (1706 $cm^{-1}$) of free isobutyric acid [Fig. 4(a)] is shifted to lower wavenumbers (1540–1590 $cm^{-1}$) on complexation with Al [Figs. 4(b) and (c)], as expected for organic acid salts. The peak [Figs. 4(b) and (c)] at 3670 $cm^{-1}$ ($\nu_{O-H}$) indicates the presence of $Al(OH)(O_2CiPr)_2$ as corroborated by comparison with an authentic sample [Fig. 4(b)] prepared by reaction of $Al(OH)_3$ with isobutyric acid and isobutyric anhydride, reaction (3).[27] Although efforts were made to limit sample exposure to humidity, it is likely that samples adsorb traces of moisture during transfer from the glove-box to the IR sample chamber, resulting in some hydrolysis. Note that DRIFTS preferentially shows the sample surface that is exposed most during sample transfer.

The small peak at 1706 $cm^{-1}$ in the DRIFTS of aluminum isobutyrates (Figs. 4(b) and (c)) corresponds to the $\nu_{C=O}$ of trace amounts of free isobutyric acid.[26] This contaminant does not influence the final ceramic product, as all the organic

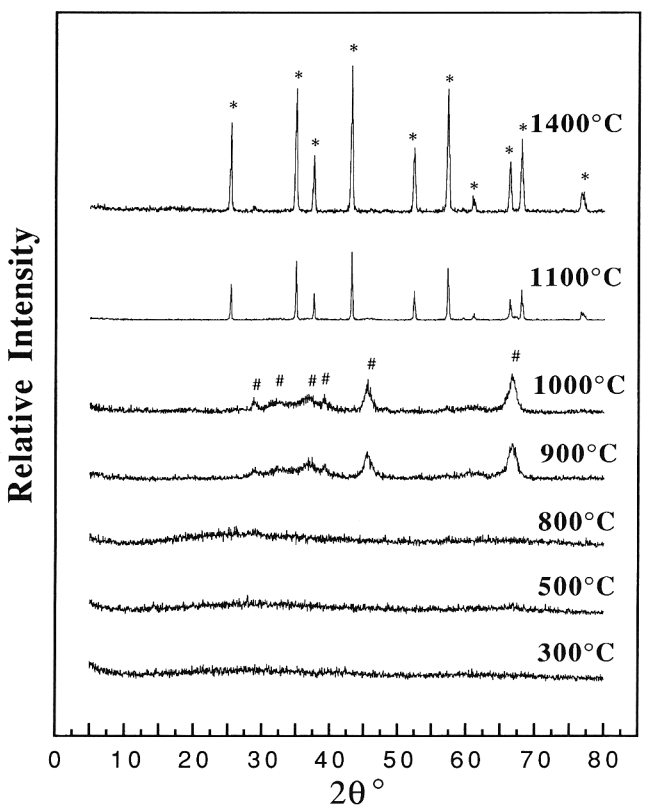


**Fig. 3.** XRD of aluminum isobutyrate pyrolyzed at selected temperatures. The samples were ramped at 5°C/min in air to selected temperatures followed by a 2 h hold at temperature. The peaks with "*" correspond to α-alumina phase JCPDS file 10-173, and "#" corresponds to η-alumina phase JCPDS file 4-875.

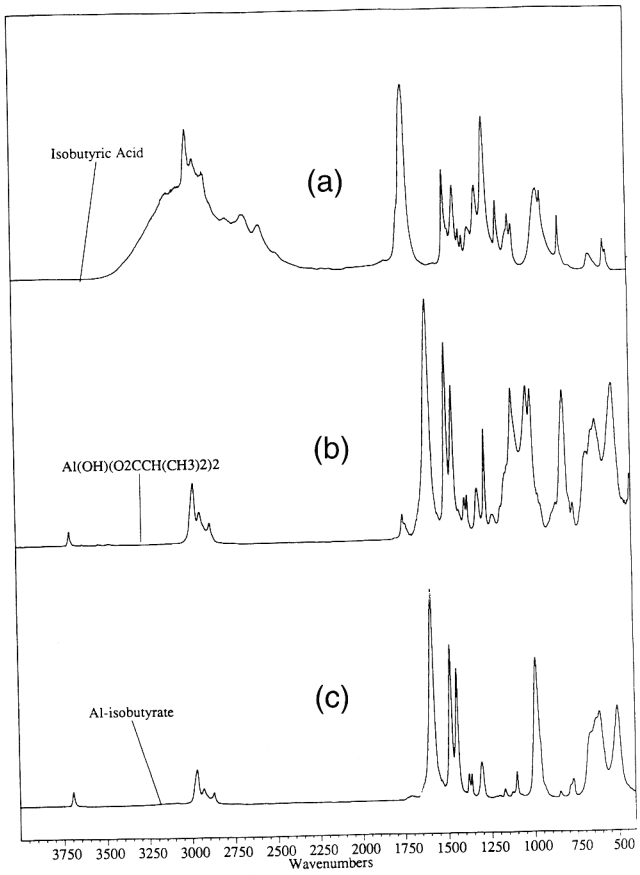


**Fig. 4.** DRIFTS of (a) isobutyric acid, (b) $Al(OH)(O_2CiPr)_2$, and (c) $Al(O_2CiPr)_3$.

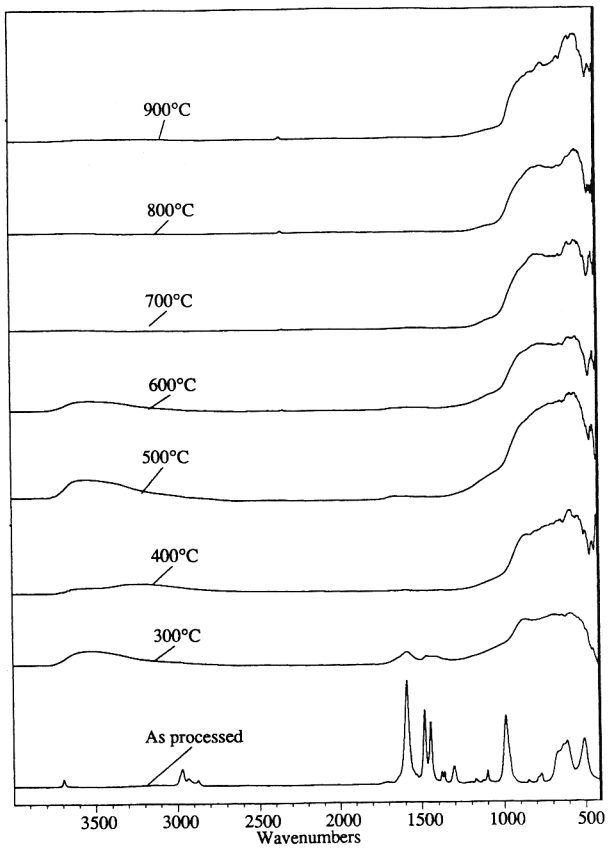


**Fig. 5.** DRIFTS of $Al(O_2CiPr)_3$ pyrolyzed to selected temperatures. Samples were ramped at 5°C/min in air to selected temperatures followed by a 2 h hold at temperature.

ligands and Al–OH groups are eliminated during pyrolysis. $Al(O_2CiPr)_3$ was also characterized by NMR (see below).

DRIFT spectra of $Al(O_2CiPr)_3$ heated to selected temperatures at 5°C/min for 2 h (Fig. 5) complement the XRD and TGA/DTA studies providing a view of the transformations at the atomic scale. In Fig. 5, the spectra show that on heating to 300°C, the peaks at 3670 $cm^{-1}$ ($\nu_{O-H}$), 2887, 2945, and 2978 $cm^{-1}$ ($\nu_{C-H}$), and at 1588, 1477, and 1448 $cm^{-1}$ ($\nu_{C=O}$) are eliminated. The resulting spectra are indicative of an amorphous, inorganic material.

In the 300°C spectrum, new peaks appear at 1465 and 1585 $cm^{-1}$. These bands are in positions identical to carbonate bands seen for all of the group I and II metal carbonates,[30,31] and therefore suggest the formation of a carbonate species. However, as pointed out by a referee, simple aluminum carbonate, e.g., $Al_2(CO_3)_3$, has not been described in the literature. However, commercial aluminum hydroxide [$Al(OH)_3$, Aldrich] comes with a label that indicates that it absorbs $CO_2$, and indeed, the FTIR of the as-received material also exhibits the same bands which remain even on heating to 300°C. Furthermore, thermal decomposition of aluminum formate, $Al(O_2CH)_3$, under similar conditions, also produces the same traces of carbonate species.[32] Thus, we presume that some form of aluminum carbonate species is produced that is relatively stable (see below). However, the absence of a powder diffraction pattern in the XRD suggests that the carbonate is amorphous, of insufficient quantity to register (less than 2%), or that the crystallite sizes are small. Because the peak intensities are relatively weak, it is likely that very little carbonate forms.

The carbonate bands disappear on heating to 500°C, indicating decomposition of the carbonate, in accord with previous studies.[29] The only other absorption bands of note are those attributable to surface Al–OH groups ($\nu_{O-H}$, 3200–3400 $cm^{-1}$) which are present in the spectra up to 600°C. These groups disappear on heating to 700°C. No corresponding weight change occurs in the TGA, which supports the assignment as surface species. The DRIFT spectra change very little above 700°C, indicating that atomic-level reorganization is complete by this temperature.

*(D) Nuclear Magnetic Resonance Studies:* $^1H$ and $^{13}C$ solution NMR were used to confirm the solution structures of both metal carboxylates. As can be seen in Table II, the proton and carbon peak positions and proton coupling patterns are nearly identical. Indeed, comparison with literature values, especially with our previous work on other isobutyrates,[6] shows almost no deviation in peak positions or coupling patterns for a wide variety of metal isobutyrates. Thus, there are no definitive differences that require further comment.

**Table I. Selected DRIFTS Data for $Al(O_2CiPr)_3$ and $Y(O_2CiPr)_3$[†]**

| Isobutyrate | $\nu_{C-H}$ ($cm^{-1}$) | $\nu_{COO}$[‡] ($cm^{-1}$) | $\nu_{COO}$[§] ($cm^{-1}$) |
|---|---|---|---|
| $Al(O_2CiPr)_3$ | 2978, 2945, 2887 | 1588 | 1477, 1448 |
| $Y(O_2CiPr)_3$[¶] | 2974, 2934, 2875 | 1540 | 1477, 1430 |
| $Me_2CHCO_2H$ | 2979, 2940, 2882 | 1706 | 1477, 1416 |

[†]The data reported are specific, strong absorption bands for the anhydrous, acid-free complexes and are not meant to be comprehensive. Accuracy is ±2.5 $cm^{-1}$. [‡]Antisymmetric stretch. [§]Symmetric stretch. [¶]From Ref. 6.

**Table II. $^{1}H$ and $^{13}C$ NMR Spectra for $Al(O_2CiPr)_3$ and $Y(O_2CiPr)_3$**

| | $^{1}H^{\dagger,\ddagger,\S}$ | | $^{13}C^{\dagger,\S}$ | | |
|---|---|---|---|---|---|
| Isobutyrate | $H^2$ | $H^3$ | $C^1$ | $C^2$ | $C^3$ |
| $Al(O_2CiPr)_3$ | 2.33 (sep) | 1.02 (d) | 182.9 | 35.2 | 18.8 |
| $Y(O_2CiPr)_3$ | 2.24 (sep) | 0.99 (d) | 187.0 | 34.9 | 19.3 |

†NMRs taken in DMSO-$d_6$ using TMS as an internal standard. ‡d: doublet; sep: septet. §$C^1$–$C^3$ (hydrogens labeled by carbon position): $M[O_2C^1C^2H(C^3H_3)_2]_3$.

### *(3) Synthesis of $Y(O_2CiPr)_3$*

Yttrium isobutyrate was synthesized according to reaction (6) using published procedures:[6]

$$Y + 3Me_2CHCO_2H \xrightarrow{\text{trace } HgCl_2/THF \text{ reflux}} 1.5H_2\uparrow + Y(O_2CiPr)_3 \quad (6)$$

### *(4) Characterization of $Y(O_2CiPr)_3$*

*(A) Thermal Analyses:* Under the conditions studied here and in Ref. 6, $Y(O_2CiPr)_3$ decomposes thermally as shown below:

$$Y(O_2CR)_3 \xrightarrow{\approx 400°C} Y_2O_3 + Y_2(CO_3)_3 \text{ (minor)} + \text{gases}$$
$$(CO_2 + H_2O + \text{propene} + \text{other})\uparrow \quad (7)^6$$

The TGA profile (Fig. 6) is rather straightforward with a single mass loss occurring between 260° and 360°C, corresponding to oxidative decomposition of the complex. The DTA (Fig. 7) also exhibits a single major event in the same temperature range. Above 360°C, the TGA indicates a slow, minor mass loss corresponding to loss of residual carbon as $CO_2$ (see DRIFTS studies), ≈7%. The ceramic yield for $Y(O_2CiPr)_3$ is 32% (Fig. 6), exactly as calculated for $Y(O_2CiPr)_3$, given reaction (7).

*(B) DRIFTS:* Figure 8 displays DRIFTS spectra for $Y(O_2CiPr)_3$ heated to selected temperatures (5°C/min in dry air) for 2 h. Peak positions for selected absorptions are recorded in Table I. Reference 6 provides more details. As with the $Al(O_2CiPr)_3$ studies, the DRIFTS studies provide a view of the transformations at the atomic scale. The spectrum of $Y(O_2CiPr)_3$ (Fig. 8) is very similar to that of the Al complex, showing $\nu_{C-H}$ bands at 2875, 2934, and 2974 $cm^{-1}$, and $\nu_{C=O}$ bands at 1430, 1477, and 1540 $cm^{-1}$. Likewise, $Y(O_2CiPr)_3$ decomposes on heating to 300°C with concomitant formation of new peaks at 1404 and 1520 $cm^{-1}$, indicative of carbonate species, e.g., $Y_2(CO_3)_3$. The carbonate band intensities are greater relative to those observed in the Al isobutyrate decomposition. Furthermore, these peaks remain when samples are heated to temperatures ≤800°C; although the intensities diminish as expected based on the slow but continuous weight loss observed in the TGA from 500° to 800°C. This weight loss amounts to only 0.1% of the total mass loss observed above 800°C, indicating 0.1 wt% carbonate remained in the material.

As in the $Al(O_2CiPr)_3$ decomposition, Y–OH peaks appear in the region 3100–3600 $cm^{-1}$, coincident with formation of the carbonate species. These peaks also persist to 800°C, but diminish in intensity as the pyrolysis temperature increases. In both instances, it is assumed that the Y–OH peaks are lost through a surface diffusion process that eventually leads to evolution of $H_2O$.

A sharp peak appears at 560 $cm^{-1}$ in the 300°C DRIFTS sample and grows in intensity at higher temperatures. This peak corresponds to $\nu_{Y-O}$ and indicates formation of localized crystallinity,[29] as discussed in the XRD section. In contrast, the XRD powder patterns show no evidence for formation of crystalline carbonate species.

*(C) X-ray Powder Diffraction (XRD) Patterns:* Figure 9 displays XRD powder patterns for $Y(O_2CiPr)_3$ pyrolysis samples produced in the same manner as used in the DRIFTS studies. At 300° and 350°C, the broad peaks in the resulting powder patterns (intensities enhanced 8 times) indicate that the material starts to crystallize at relatively low temperatures. At 500°C, the pattern clearly shows crystalline bcc yttria; however, the broad peaks and poor intensities suggest that considerable material is either amorphous or nanocrystalline.[33] It is possible that the presence of a carbonate phase inhibits crystallization; however, no evidence exists to support this conjecture. Although most of the carbonate material decomposes (by DRIFTS) by 800°C, and the remaining material is assumed to be stoichiometric $Y_2O_3$, the continued low intensities and broad

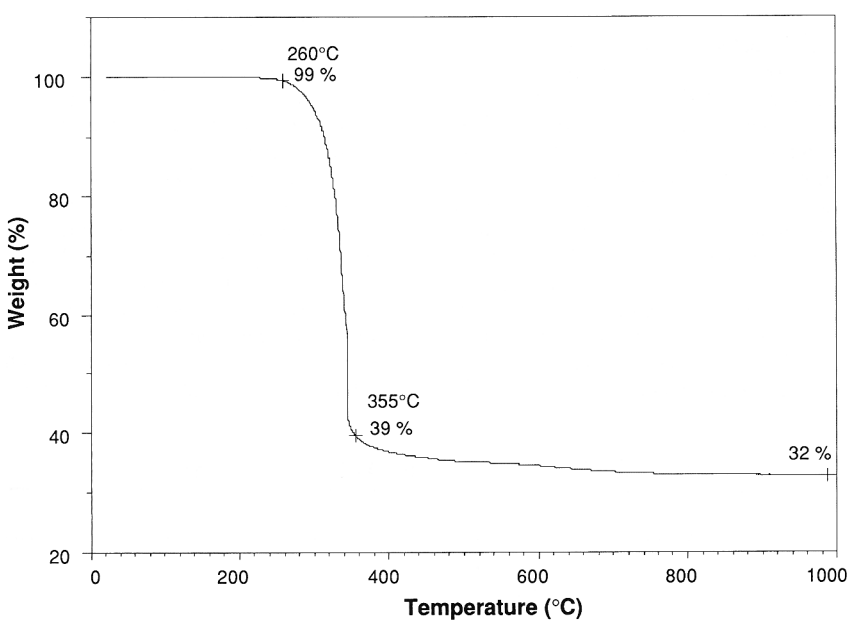


**Fig. 6.** TGA of $Y(O_2CiPr)_3$. Heated at 5°C/min to 1000°C in air.

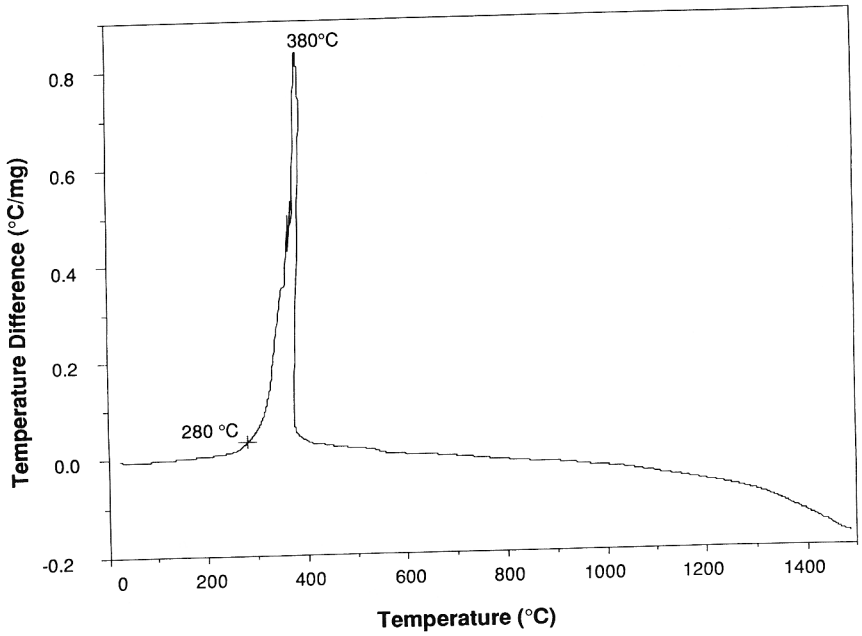


**Fig. 7.** DTA of $Al(O_2CiPr)_3$. Heated at 5°C/min to 1500°C in air.

peaks in the powder pattern still indicate a poorly crystalline material. Indeed, only by heating to 1400°C is a well-defined pattern obtained with high relative peak intensities.

### *(5) Characterization of a YAG Precursor Mixture, $5Al(O_2CiPr)_3$:$3Y(O_2CiPr)_3$*

The YAG precursor was prepared by THF dissolution of the correct stoichiometric mixture followed by vacuum removal of solvent and grinding of the resulting powder, as detailed in the experimental section. Samples of this bulk powder were then pyrolyzed to selected temperatures using the same procedures as used for the individual compounds.

*(A) Thermal Analyses:* The Fig. 10 TGA of the bulk, dry powder (5°C/min/air) appears to show a decomposition profile that is simply a superposition of both Al and Y isobutyrate decompositions. The initial mass loss would then correspond to partial hydrolytic decomposition of the Al fraction and the remaining major mass loss would then result from the primary decomposition of both types of isobutyrates. Indeed, the DTA shown in Fig. 11 shows a small exotherm in the range 270–

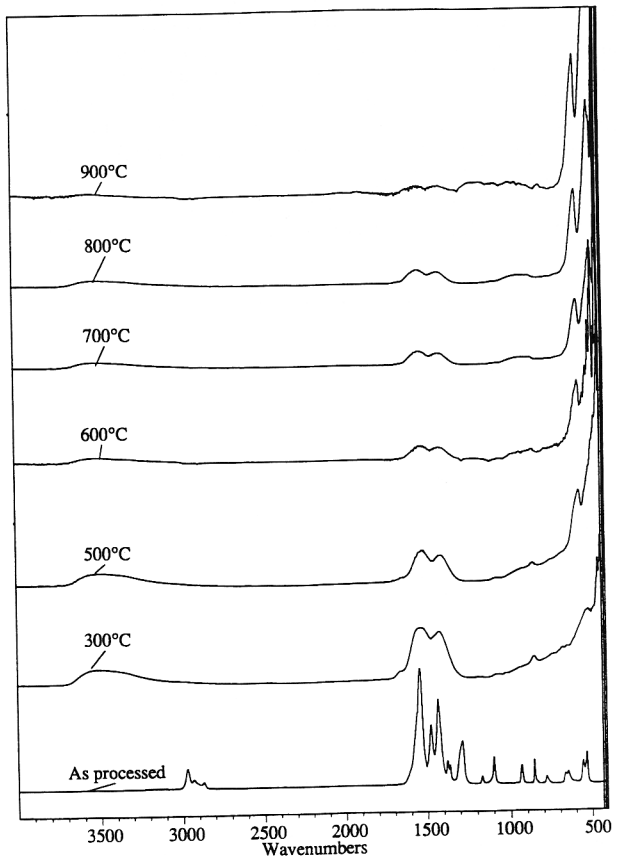


**Fig. 8.** DRIFTS of $Y(O_2CiPr)_3$ pyrolyzed to selected temperatures. The samples were ramped at 5°C/min to selected temperatures followed by a 2 h hold at temperature.

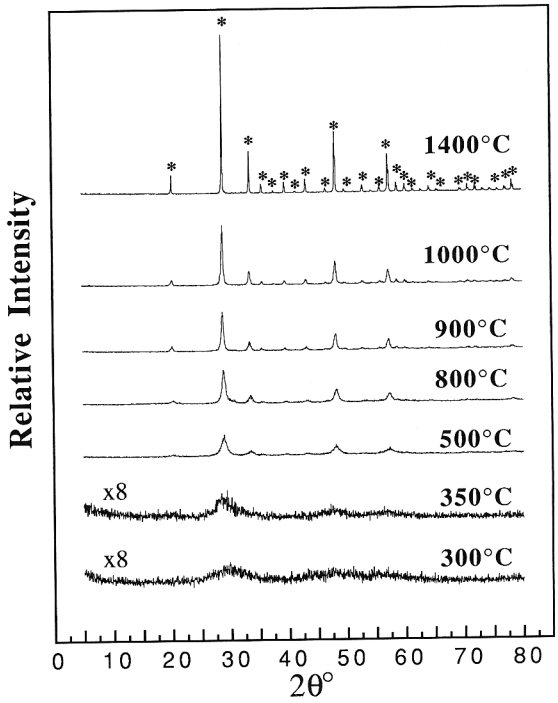


**Fig. 9.** XRD of $Y(O_2CiPr)_3$ pyrolyzed at selected temperatures. Samples were prepared as in DRIFTS studies. The peaks with "*" correspond to bcc yttria phase JCPDS file 41-1105.

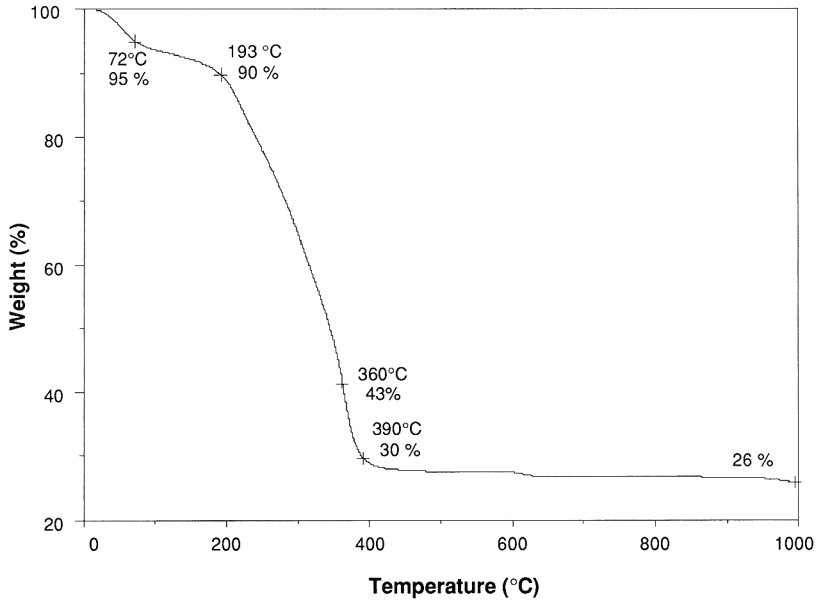


**Fig. 10.** TGA of YAG precursor. Heated at 5°C/min to 1000°C in air.

290°C that exactly parallels an event observed in the Fig. 2 DTA for $Al(O_2CiPr)_3$ decomposition.

Such behavior might be anticipated if solvent removal provided a fine-grained, physical (segregated) mixture of the two isobutyrates and both compounds decomposed independently of the other. However, on careful inspection, a major fraction of the mass loss (≈17%) occurs above 360°C, which is above both of the major mass loss events for the individual compounds. Although not definitive, this result suggests the formation of a multimetallic isobutyrate complex, as observed previously.[6] However, mass spectral fragmentation studies of the individual components and the YAG precursor show that the YAG precursor is indeed simply a very homogeneous mixture of the two components.[32] The found ceramic yield is 26%, which corresponds closely to the calculated ceramic yield expected for the 5:3 mixture, 25%.

Because the DTA (Fig. 11) does not provide details about high-temperature phase transformations [see discussion on $Al(O_2CiPr)_3$ DTA], fresh sample was first pyrolyzed to 500°C for 2 h, then identical amounts of sample and reference (20 mg each) were used to run the DTA at 5°C/min to 1500°C to obtain the inset in Fig. 11. The inset shows one exotherm in the range of 910–950°C which appears to correspond to the crystallization of YAG. This is confirmed by the XRD data (Fig. 12), shown below, which indicate formation of YAG (JCPDS File 33-40) alone.

*(B) DRIFTS:* Spectra of as-processed YAG precursor and precursor heated to selected temperatures are shown in Fig. 12. The DRIFT spectrum of as-processed YAG precursor (bottom, Fig. 12) looks like an overlap spectrum constructed from spectra of the Al and Y isobutyrates. Again, it appears that no significant intermolecular interactions occur when $Al(O_2CiPr)_3$ and $Y(O_2CiPr)_3$ are mixed in solution. The spectra of as-prepared YAG precursor shows peaks at 3690 $cm^{-1}$ ($\nu_{AlO-H}$), 2971, 2932, and 2872 $cm^{-1}$ ($\nu_{C-H}$), and at 1583, 1559, 1477, 1442, and 1433 $cm^{-1}$ ($\nu_{C=O}$).

However, on pyrolysis, the resulting materials do not behave as the individual isobutyrates. At 300°C, all of the organic

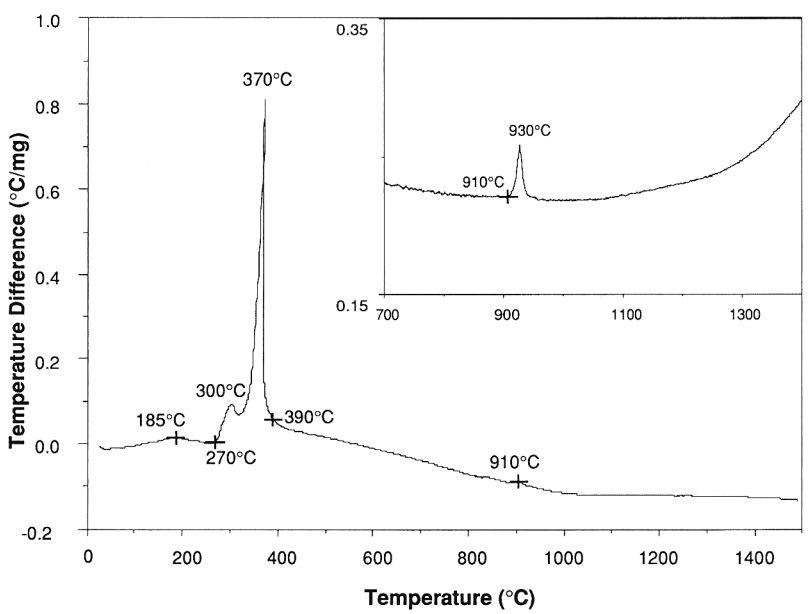


**Fig. 11.** DTA of YAG precursor. Heated at 5°C/min to 1500°C in air.

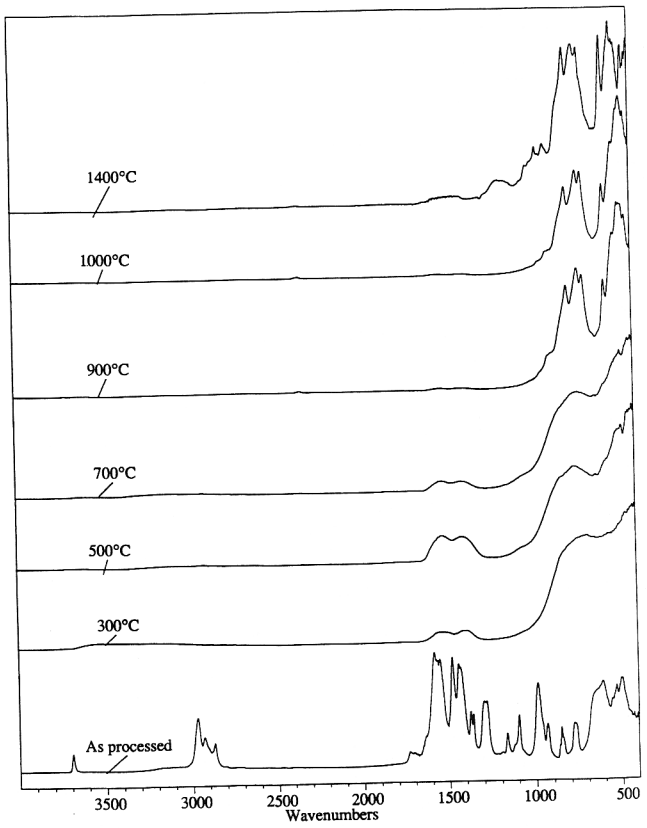


**Fig. 12.** DRIFT spectra of YAG precursor pyrolyzed to selected temperatures. Samples were heated at 5°C/min to selected temperature followed by a 2 h hold at temperature.

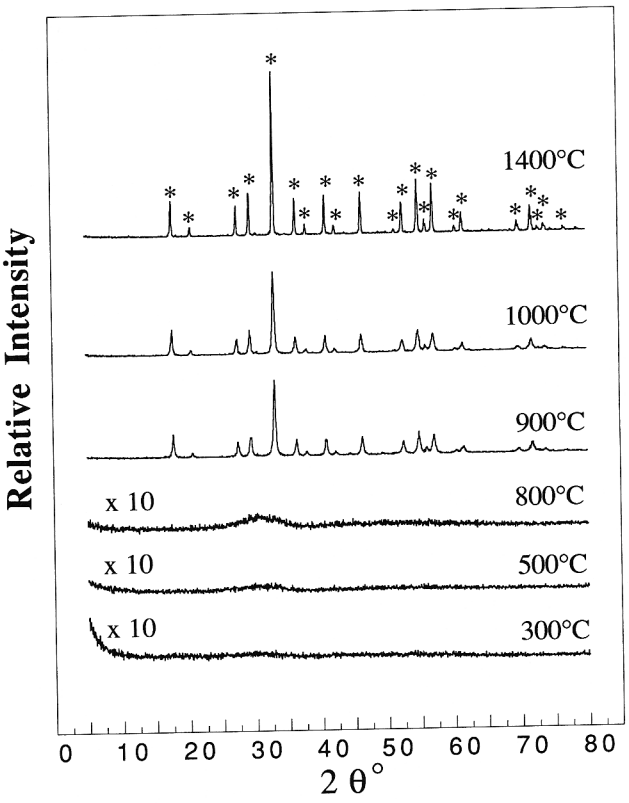


**Fig. 13.** XRD of YAG precursor pyrolyzed to selected temperatures. Samples were treated as in DRIFT studies. The peaks with "*" correspond to YAG phase JCPDS file 33-40.

ligand peaks disappear to be replaced by carbonate peaks centered at 1530 and 1400 $cm^{-1}$. A barely detectable $\nu_{O-H}$ peak is observed in the 300°C spectrum but not at higher temperatures. The carbonate peaks persist to only 700°C; however, no evidence is found at low temperatures for a sharp $\nu_{Y-O}$ peak at 560 $cm^{-1}$ (300–700°C), which supports the above statement concerning the initial exotherm in the DTA and is corroborated by the lack of a bcc yttria pattern in the XRD studies. In addition, a broad peak at 650–1000 $cm^{-1}$, found initially in the 300°C spectrum, is not found in spectra of Al or Y isobutyrate samples heated to any temperature. This peak persists to 700°C and then evolves into four peaks at ≈560, 690, 720, and 790 $cm^{-1}$ at 900°C and above. These four peaks correspond to the formation of crystalline YAG.[29] These observations provide evidence for the homogeneity of the THF derived YAG precursor.

*(C) X-ray Powder Diffraction Patterns:* XRDs of bulk pyrolysis samples are shown in Fig. 13. No intermediate crystalline phases such as bcc $Y_2O_3$, η- or α-alumina are observed before crystallization of YAG, which starts at ≈910°C (from DTA). Above 910°C, YAG continues to crystallize as evidenced by continued refinement in peak shapes and intensities. It should be noted that the XRD data were obtained for samples held at temperature for 2 h, while the DTA data were obtained for samples heated continuously to 1500°C. Thus, the exothermic crystallization peak in the DTA occurs at a higher temperature than the temperature where crystallization is first observed in the XRD studies. Additional studies show that samples held at 900°C for 5 min give XRD patterns identical to the 800°C sample in Fig. 13. However, samples held at 900°C for 15 min, or 910°C for 5 min, give well-developed, crystalline YAG.

The XRD patterns for 500° and 800°C exhibit broad features (300°, 500°, and 800°C XRDs multiplied 10 times), suggesting some local ordering as also implied by the broad peak at 650–1000 $cm^{-1}$ in the DRIFTS spectra for these same temperatures. This type of phenomena has been described as "noncrystalline, but not completely amorphous."[5b] It appears from the DRIFTS data that some form of short-range order or nucleation exists in the temperature range between 500° and 900°C. One possible interpretation is that at these temperatures the local environment is YAG, but diffusion rates are so slow that crystallization does not occur until the rates become significant, e.g., just below 900°C, based on the 900°C XRD powder pattern.

The simplicity of the observed XRD patterns is at odds with what is observed in the individual precursor pyrolysis studies, i.e., given that in the Y isobutyrate pyrolysis studies, $Y_2O_3$ crystallization starts at 300°C. These results strongly support our contention that good atomic mixing is obtained through the use of carboxylate precursors.

*(D) Density and Volume Changes:* To successfully process fully dense, defect-free, polycrystalline YAG fibers, the experimental design must allow for the extreme changes in volume and density that occur as a green, precursor fiber is transformed into a ceramic fiber. Thus, once a well-defined precursor was developed, the next step was to clearly define the desired density and volume changes.

The densities of sets of cold compacted disks of the individual compounds, $Al(O_2CiPr)_3$ and $Y(O_2CiPr)_3$, and the YAG precursor were determined and recorded in Table III. The measured densities of the individual isobutyrates can be used to calculate the density of a compacted disk with a 5:3 stoichiometry. The calculated density is 1.21 $g/cm^3$. The found density for the YAG precursor was 1.14 $g/cm^3$ (Table III) while the reported density for YAG is 4.5 $g/cm^3$. The theoretical volume change resulting from both mass loss and densification is 90%. If the precursor material is shaped as a fiber, and all of the volume change occurs only in the diametrical dimension, and full densification is obtained, the expected change in diameter will be 68%. The extensive volume changes coupled with the release of gaseous products will be the main reasons for loss of fiber integrity, as green fiber is converted to ceramic fiber. Thus, extreme care in controlling gas evolution is necessary for

**Table III. Densities of $Al(O_2CiPr)_3$, $Y(O_2CiPr)_3$ and YAG Precursor**

| Isobutyrate | Weight† (g) | Pellet diameter†,‡ (cm) | Length† (cm) | Volume† ($cm^3$) | Density ($g/cm^3$) |
|---|---|---|---|---|---|
| $Al(O_2CiPr)_3$ | 1.94 | 1.28 | 1.33 | 1.70 | 1.14 |
| $Y(O_2CiPr)_3$ | 2.04 | 1.28 | 1.21 | 1.55 | 1.31 |
| YAG precursor | 2.13 | 1.28 | 1.46 | 1.87 | 1.14 (1.21§) |

†Values are average of three measurements for each sample. ‡The pellets are processed as described in the experimental section. §The found densities of the yttrium and aluminum isobutyrates permit calculation of a theoretical density for the YAG precursor of 1.21 $g/cm^3$.

successful processing. Future papers will detail efforts to process fully dense, polycrystalline fibers with fiber diameters <20 μm.[34] Efforts to control grain sizes and grain size distributions will also be described.

## IV. Conclusions

The decomposition patterns that occur during the pyrolytic transformation of bulk samples of $Al(O_2CiPr)_3$ and $Y(O_2CiPr)_3$ to their respective, common high-temperature ceramic forms—α-alumina and bcc yttria—were examined. The results established baseline behavior patterns of potential use in evaluating the decomposition patterns of a YAG precursor formulated from 5:3 stoichiometric mixtures of $Al(O_2CiPr)_3$ and $Y(O_2CiPr)_3$ dissolved in THF and recovered by vacuum evaporation of solvent. In the individual cases, decomposition followed well-defined pathways wherein the initial products were the amorphous oxides contaminated with trace to minor amounts of carbonate species. At higher temperatures, the ceramic products crystallized, first η-alumina (840°C) and then α-alumina (>1100°C), for $Al(O_2CiPr)_3$ and only bcc yttria (≥300°C) for $Y(O_2CiPr)_3$. Surprisingly, these results had almost no bearing on the reactivity pattern of the YAG precursor which behaved like a separate compound and decomposed only to crystalline YAG at ≈910°C without any conclusive evidence of phase separation.

**Acknowledgment:** We would like to thank the referees for useful comments and suggestions.

## References

[1]G. S. Corman, "High-Temperature Creep of Some Single Crystal Oxides," *Ceram. Eng. Sci. Proc.*, **12**, 1745–66 (1991).

[2]E. M. Levin, C. R. Robbins, and H. F. McMurdie, *Phase Diagrams for Ceramists*; p. 122. Edited by M. K. Reser. American Ceramic Society, Columbus, OH, 1969.

[3]T. A. Parthasarathy, T. Mah, and K. Keller, "High-Temperature Deformation Behavior of Polycrystalline Yttrium Aluminum Garnet (YAG)," *Ceram. Eng. Sci. Proc.*, **12** [9–10] 1767–73 (1991).

[4]A. H. Chokshi and J. R. Porter, "Analysis of Concurrent Grain Growth During Creep of Polycrystalline Alumina," *J. Am. Ceram. Soc.*, **69** [2] C-37–C-39 (1986).

[5](a) G. Gowda, "Synthesis of Yttrium Aluminates by the Sol–Gel Process," *J. Mater. Sci. Lett.*, **5**, 1029–32 (1986). (b) R. S. Hay, "Phase Transformations and Microstructure Evolution in Sol–Gel Derived Yttrium–Aluminum Garnet Films," *J. Mater. Res.*, **8**, 578–604 (1993).

[6](a) R. M. Laine, K. A. Youngdahl, R. A. Kennish, M. L. Hoppe, Z.-F. Zhang, and D. J. Ray, "Superconducting Fibers from Organometallic Precursors, Part II: Chemistry and Low Temperature Processing," *J. Mater. Res.*, **6**, 895–907 (1991). (b) Z.-F. Zhang, R. A. Kennish, K. A. Blohowiak, M. L. Hoppe, and R. M. Laine, "Superconducting Fibers from Organometallic Precursors, Part III: High Temperature Pyrolytic Processing," *J. Mater. Res.*, **8**, 1777–90 (1993). (c) R. M. Laine and K. A. Youngdahl, U.S. Pat. No. 5 071 833, 1993.

[7]R. C. Mehrotra, "Polymetallic Alkoxides—Precursors for Ceramics"; pp. 81–92 in Materials Research Society Symposia Proceedings, Vol. 121, *Better Ceramics Through Chemistry III*. Edited by C. J. Brinker, D. E. Clark, and D. R. Ulrich. Materials Research Society, Pittsburgh, PA, 1988.

[8](a) J. Livage, M. Henry, and C. Sanchez, "Sol–Gel Chemistry of Transition Metal Oxides," *Prog. Solid State Chem.*, **18**, 259–341 (1988). (b) I. M. Thomas, "Multicomponent Glasses from the Sol–Gel Process"; pp. 2–15 in *Sol–Gel Technology for Thin Films, Fibers, Preforms, Electronics, and Specialty Shapes*. Edited by L. Klein. Noyes, Park Ridge, NJ, 1988.

[9]H. Dislich, "Glassy and Crystalline Systems from Gels: Chemical Basis and Technical Application," *J. Non-Cryst. Solids*, **57**, 371–88 (1983).

[10]C. Gerardin, S. Sundaresan, J. Benziger, and A. Navrotsky, "Structural Investigation and Energetics of Mullite Formation from Sol–Gel Precursors," *Mater. Chem.*, **6**, 160 (1994).

[11]L. C. Klein, "Sol–Gel Processing of Silicates," *Annu. Rev. Mater. Sci.*, **15**, 227–48 (1985).

[12]L. Bonhomme-Coury, F. Babonneau, and J. Livage, "Comparative Study of Various Sol–Gel Preparations of Cordierite Using $^{27}Al$ and $^{29}Si$ Liquid- and Solid-State NMR Spectroscopy," *Chem. Mater.*, **5**, 323–30 (1993).

[13]T. Fukui, C. Sakura, and M. Okuyama, "Effect of Prehydrolysis on the Structure of a Complex Alkoxide as a Cordierite Precursor and Their Crystallization Behavior," *J. Non-Cryst. Solids*, **162**, 178–87 (1993).

[14]Z.-F. Zhang, *Fabrication of High $T_c$ Superconducting Fibers from Organometallic Precursors*"; Master's Thesis. University of Washington, Seattle, WA, 1990.

[15]J. C. Bailar, Jr., H. J. Emeleus, R. Nyholm, and A. F. Trotman-Dickenson, *Comprehensive Inorganic Chemistry*; pp. 1046–47. Pergamon Press, New York, 1973.

[16]C. F. Baes, Jr., and R. E. Mesmer, *The Hydrolysis of Cations*; pp. 112–23. Wiley-Interscience, New York, 1976.

[17]K. Nakamoto, *Infrared and Raman Spectra of Inorganic and Coordination Compounds*, 4th ed. Wiley-Interscience, New York, 1986.

[18]B. M. Gatehouse, S. E. Livingstone, and R. S. Nyholm, "The Infrared Spectra of Some Simple and Complex Carbonates," *J. Chem. Soc.*, 3137–42 (1958).

[19]E. Spinner, "The Vibration Spectra of Some Substituted Acetate Ions," *J. Chem. Soc.*, 4217–26 (1964).

[20]J. Fujita, A. E. Martell, and K. Nakamoto, "Infrared Spectra of Metal Chelate Compounds. VIII. Infrared Spectra of Co(III) Carbonato Complexes," *J. Chem. Phys.*, **36**, 339 (1962).

[21]A. I. Grigor'ev, "Infrared Absorption Spectra of Acetates of Elements in Groups I and II of the Periodic System," *Russ. J. Inorg. Chem. (Engl. Transl.)*, **8**, 409–14 (1963).

[22]A. I. Grigor'ev and V. N. Maksimov, "Infrared Absorption Spectra of Acetates of Group III Metals and Their Hydrate," *Russ. J. Inorg. Chem. (Engl. Transl.)*, **9**, 580–82 (1964).

[23]J. D. Donaldson, J. F. Knifton, and S. D. Ross, "The Effect of the Lone Pair on the Infrared Spectra of Some Main Group Acetates," *Spectrochim. Acta*, **21**, 275–77 (1965).

[24]J. D. Donaldson, J. F. Knifton, and S. D. Ross, "The Vibrational Spectra of Some Tin(II) Carboxylate Complexes," *Spectrochim. Acta*, **21**, 1043–1046 (1965).

[25]A. V. R. Warrier and P. S. Narayanan, "Infrared Spectra of Crystalline Chloroacetates of Cu, Ca, Sr, Ba, and Pb," *Spectrochim. Acta*, **23A**, 1061–67 (1967).

[26]A. V. R. Warrier and R. S. Krishnan, "Infrared Spectra of Trichloroacetates of Copper, Calcium, Strontium and Barium," *Spectrochim. Acta*, **27A**, 1243–46 (1971).

[27]A. L. Mckenna, "Aluminum Carboxylates," *Encyclopedia of Chemical Technology*, 4th ed., Vol. 2; pp. 273–81. Edited by L. Gray, L. J. Humphreys, M. Howe-Grant, and J. I. Kroschwitz. Wiley Interscience, New York, 1991.

[28]D. L. Pavia, G. M. Lampman, and G. S. Kriz, Jr., *Introduction to Spectroscopy: A Guide for Students of Organic Chemistry*; pp 54–55, 68. Saunders, Philadelphia, PA, 1979.

[29]L. M. Seaverson, S.-Q. Luo, P.-L. Chien, and J. F. McClelland, "Carbonate Associated with Hydroxide Sol–Gel Processing of Yttria: An Infrared Spectroscopic Study," *J. Am. Ceram. Soc.*, **69**, 423–29 (1986).

[30]P. Kansal and R. M. Laine, "Pentacoordinate Silicon Complexes as Precursors to Silicate Glasses and Ceramics," *J. Am. Ceram. Soc.*, **77**, 875–82 (1994).

[31]P. Kansal and R. M. Laine, "Group II Tris(glycolato)silicates as Precursors to Silicate Glasses and Ceramics," *J. Am. Ceram. Soc.*, **78** [3] 529–38 (1995).

[32]Y. Liu and R. M. Laine; unpublished results.

[33]B. D. Cullity, *Elements of X-ray Diffraction*, 2nd ed.; pp. 284–85. Addison-Wesley, Reading, MA, 1978.

[34]Y. Liu, Z.-F. Zhang, J. Halloran, and R. M. Laine; unpublished work. □